Canonical microRNA loss drives tumor development implicating therapeutic efficacy of enoxacin in angiosarcoma

Bozhi Liu, Ant Murphy, Annaleigh Benton, Lauren Gartenhaus, William Budka, Juliana M. Bronzini, Samuel Hartzler, Madison E. Yates, Alejandra Romero Alzate, Nimod D. Janson, Shyaman Jayasundara, Sagar Utturkar, Nadia A. Lanman, Majid Kazemian, Jason A. Hanna

Supplemental Information Content

Supplemental Figures

Supplemental Figure S1. Enoxacin effects in AS cells.
Supplemental Figure S2. miRNA alterations with ENX.
Supplemental Figure S3. Altered miRNA abundance and processing with enoxacin.
Supplemental Figure S4. mRNA expression changes with enoxacin.
Supplemental Figure S5. Gene Set Enrichment Analysis (GSEA) in cells treated with enoxacin.

Supplemental Tables

Supplemental Table S1. Differentially expressed miRNAs in ADC106 cells treated with Enoxacin.
Supplemental Table S2. Differentially expressed miRNAs in SVR cells treated with Enoxacin.
Supplemental Table S3. Gene ontology analysis of enoxacin upregulated genes in ADC106 cells.
Supplemental Table S4. Gene ontology analysis of enoxacin upregulated genes in SVR cells.
Supplemental Table S5. Gene ontology analysis of enoxacin downregulated genes in ADC106 cells.
Supplemental Table S6. Gene ontology analysis of enoxacin downregulated genes in SVR cells.
Supplemental Table S7. Predicted miRNA regulated genes in top downregulated pathways for miRNAs with increased abundance in ADC106 cells treated with 100μM ENX.
Supplemental Table S8. Predicted miRNA regulated genes in top downregulated pathways for miRNAs with increased abundance in SVR cells treated with 100μM ENX.
Supplemental Table S9. Primers used for qRT-PCR and genotyping.
Supplemental Table S10. STR profiles of angiosarcoma cell lines.
Supplemental Table S11. Antibodies used for IHC and immunoblots.

Supplemental figure legends

Supplemental Figure S1. Enoxacin effects in AS cells. (A) Representative images of clonogenic colony formation in human AS cells treated with DMSO or 125 μM enoxacin (ENX) and corresponding quantification in main Fig. 3K. **(B)** Relative luciferase activity of miR-497 sensor reporter in HEK293T cells transfected with psiCHECK2-miR-497 sensor reporter and treated with DMSO or 100 μM ENX for 48 hours. **(C)** Relative expression of *Dicer1* (left panel) or *Tarbp2* (right panel) by qRT-PCR in mouse AS cells treated with indicated concentration of ENX for 72 hours. **(D-E)** Immunoblots for indicate proteins from lysates of ADC106 and SVR treated with 100 μM ENX for 72 hours. **(F)** Relative expression of *DICER1* (left panel) or *TARBP2* (right panel) by qRT-PCR in human AS cells treated with indicated concentration of ENX for 72 hours. **(G-H)** Immunoblots for indicate proteins from lysates of KU-CAS3 or KU-CAS5 cells treated with 125 μM ENX for 72 hours, *p<0.05, **p<0.01, ***p<0.001, ****p<0.0001.

Supplemental Figure S2. miRNA alterations with ENX. (A) MA plot of small RNA-seq data in ADC106 or **(B)** SVR cells (log_2 fold change of ENX vs. DMSO). A base mean cut-off of 10 applied as the minimum expression level. **(C)** Combined volcano plot of the -log_{10} FDR vs log_2 fold change of differentially expressed miRNAs in the ADC106 and SVR cells with the point size representing mean normalized expression (base mean). **(D)** Euler diagram of the common miRNAs increased in abundance with FDR < 0.05 and log_2 fold change > 0.5 in ENX vs. DMSO ADC106 and SVR cells. **(E)** Multivariable bubble plot of the 50 common miRNAs of increased abundance based on the mean normalized expression (base mean) and differential expression (log_2 fold change) in ADC106 (blue) and SVR (red) cells.

Supplemental Figure S3. Altered miRNA abundance and processing with enoxacin. (A) Heatmap of the commonly dysregulated miRNAs by small RNA-seq in the ADC106 and SVR cells treated with ENX or DMSO for 72 hours. **(B)** Relative expression of indicated precursor

pre-miRNA or **(C)** mature miRNAs by qRT-PCR from ADC106 cells treated with indicated concentration of ENX for 72 hours. **(D)** Relative expression of precursor or **(E)** mature miRNA in SVR cells treated as in (B),*p<0.05, **p<0.01, ***p<0.001, ****p<0.0001.

Supplemental Figure S4. mRNA expression changes with enoxacin. (A-B) Volcano plots showing -$\log_{10}$ FDR versus $\log_2$ fold change in mRNA expression in ADC106 (A) or SVR (B) cells treated with enoxacin (ENX) or DMSO for 72 hours. Genes significantly downregulated (FDR < 0.05, $\log_2$ fold change < -0.5; blue) or upregulated (FDR < 0.05, $\log_2$ fold change > 0.5; red) are highlighted. **(C)** Gene expression data from RNA-seq were z-scored normalized. Hierarchical clustering of genes (rows) and samples (columns) of consistent direction and magnitude of fold change in both cell lines (mean $|\log_2 FC| > 0.5$) included. Color scale represents relative expression (z-score). **(D)** Log_2 fold change in expression of upregulated genes in ADC106 (blue) or SVR (red) cells treated with DMSO or ENX. **(E)** Expression of downregulated angiogenic and endothelial genes in cells as in (D).

Supplemental Figure S5. Gene Set Enrichment Analysis (GSEA) in cells treated with enoxacin. (A) Bar graphs of the Normalized Enrichment (NES) scores of the top pathways from GSEA analysis of the differentially expressed genes in ADC106 or **(B)** SVR cells**. (C)** Differential expression ($\log_2$ fold change) of selected genes from the cell cycle and E2F targets gene sets in ADC106 (blue) or SVR (red) cells.

Supplemental Figure S1.

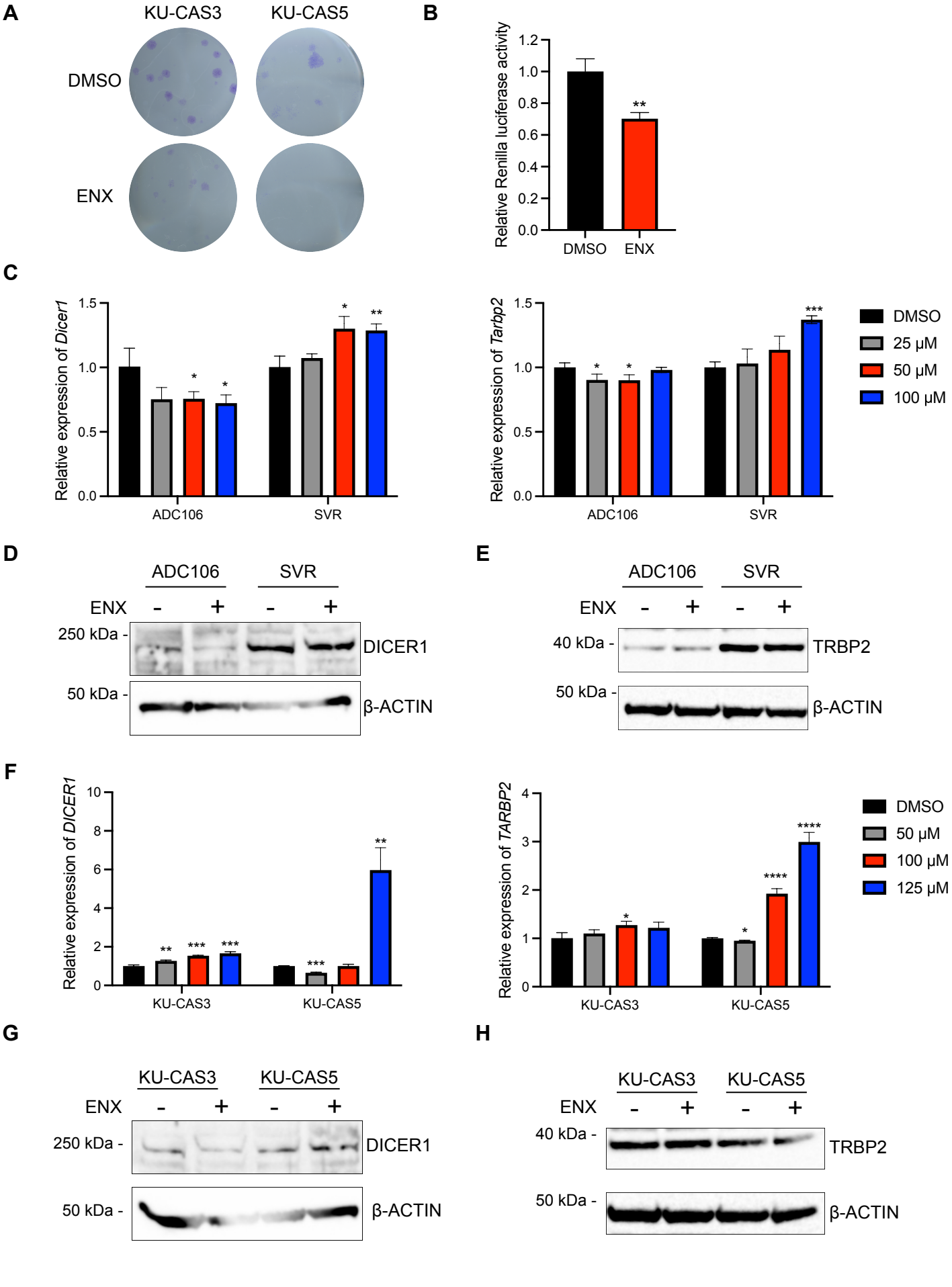

Supplemental Figure S2.

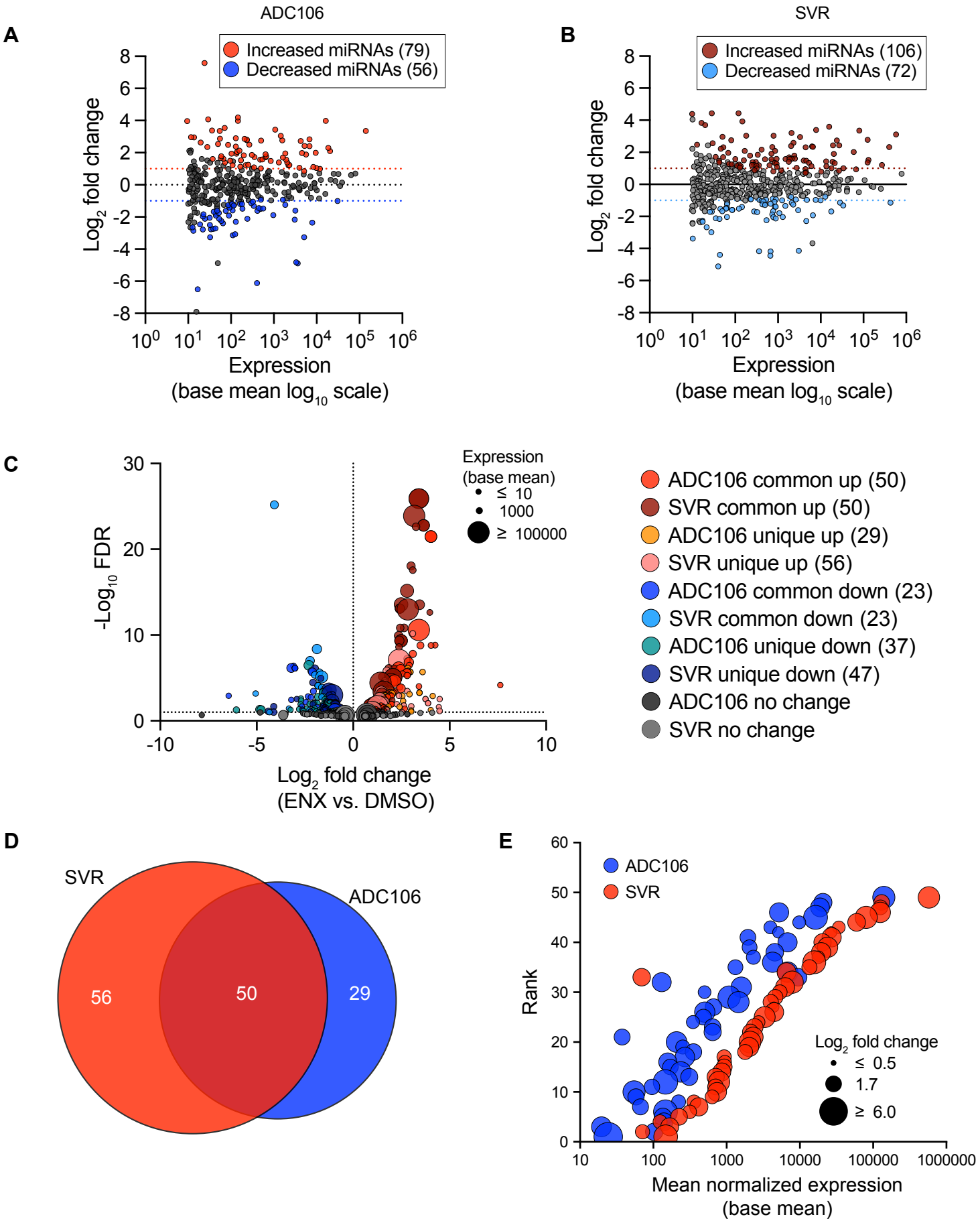

Supplemental Figure S3.

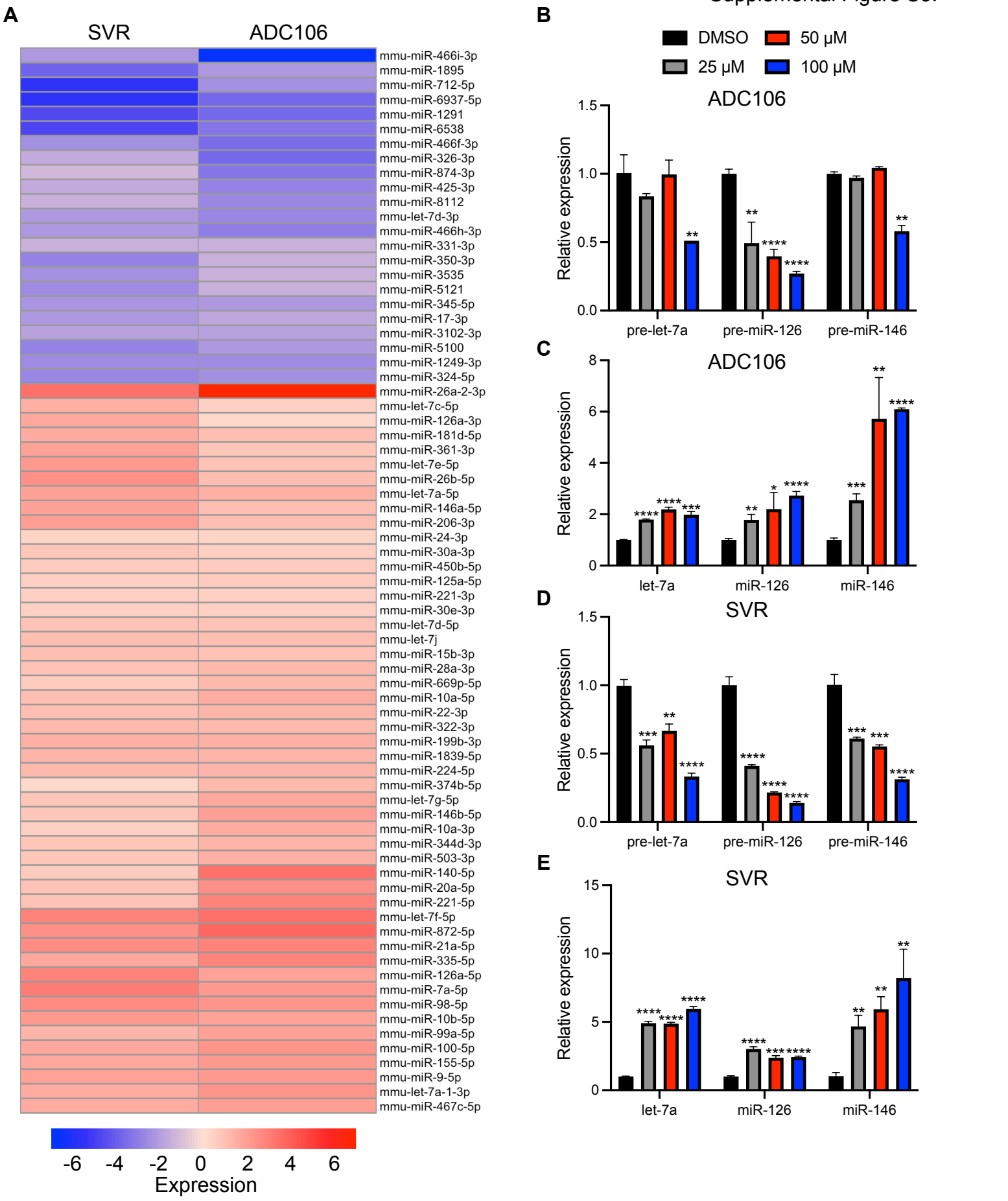

Supplemental Figure S4.

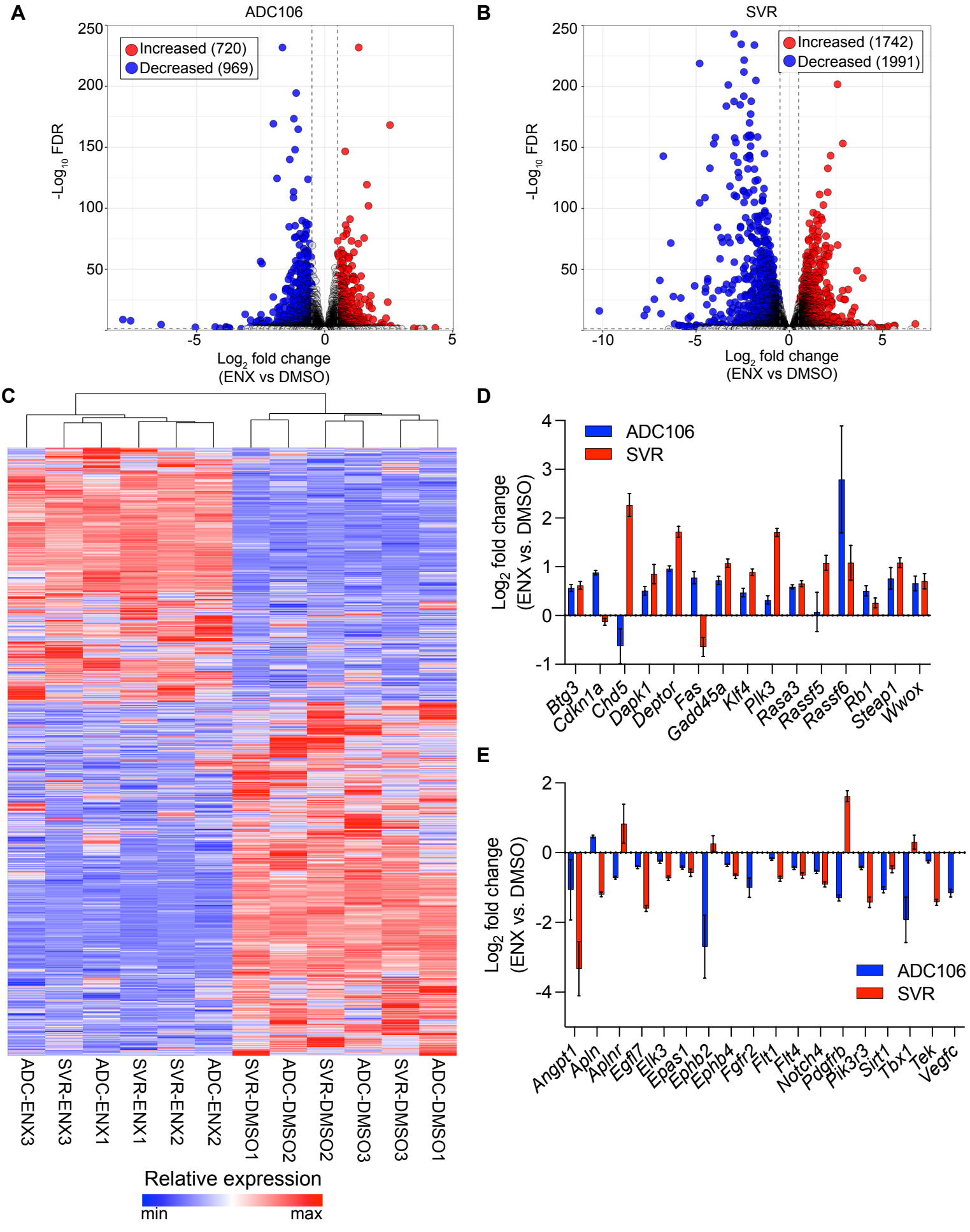

Supplemental Figure S5.